



## OPEN ACCESS

## EDITED BY

Dianming Wu,  
East China Normal University, China

## REVIEWED BY

Changlun Tong,  
Zhejiang University, China  
Zirui Liu,  
Chinese Academy of Sciences (CAS), China

## \*CORRESPONDENCE

Hongbo Fu,  
✉ fuhb@fudan.edu.cn  
Xiang Tu,  
✉ tuxiang527@163.com

<sup>†</sup>These authors have contributed equally to this work and share first authorship

RECEIVED 18 April 2024

ACCEPTED 06 May 2024

PUBLISHED 30 May 2024

## CITATION

Wang X, Han Y, Tu X, Shen J, Zhang B and Fu H (2024), Distribution of volatile organic compounds (VOCs) in the urban atmosphere of Hangzhou, East China: Temporal variation, source attribution, and impact on the secondary formations of ozone and aerosol. *Front. Environ. Sci.* 12:1418948. doi: 10.3389/fenvs.2024.1418948

## COPYRIGHT

© 2024 Wang, Han, Tu, Shen, Zhang and Fu. This is an open-access article distributed under the terms of the [Creative Commons Attribution License \(CC BY\)](https://creativecommons.org/licenses/by/4.0/). The use, distribution or reproduction in other forums is permitted, provided the original author(s) and the copyright owner(s) are credited and that the original publication in this journal is cited, in accordance with accepted academic practice. No use, distribution or reproduction is permitted which does not comply with these terms.

# Distribution of volatile organic compounds (VOCs) in the urban atmosphere of Hangzhou, East China: Temporal variation, source attribution, and impact on the secondary formations of ozone and aerosol

Xin Wang<sup>1†</sup>, Yu Han<sup>1†</sup>, Xiang Tu<sup>2\*</sup>, Jiandong Shen<sup>3</sup>, Baojun Zhang<sup>4</sup> and Hongbo Fu<sup>1,5,6\*</sup>

<sup>1</sup>Shanghai Key Laboratory of Atmospheric Particle Pollution and Prevention, Department of Environmental Science & Engineering, Institute of Atmospheric Sciences, Fudan University, Shanghai, China, <sup>2</sup>Jiangxi Key Laboratory of Environmental Pollution Control, Jiangxi Academy of Eco-Environmental Sciences and Planning, Nanchang, China, <sup>3</sup>Hangzhou Ecological Environment Monitoring Center of Zhejiang Province, Hangzhou, China, <sup>4</sup>Tangshan Ecological Environment Publicity and Education Center, Tangshan, China, <sup>5</sup>Collaborative Innovation Center of Atmospheric Environment and Equipment Technology (CICAEET), Nanjing University of Information Science and Technology, Nanjing, China, <sup>6</sup>Institute of Eco-Chongming (SIEC), Shanghai, China

Volatile organic compounds (VOCs) significantly influence air quality, atmospheric chemistry, and human health. An observational study was performed at the urban site of Hangzhou, China, to analyze VOC characteristics, sources, chemical reactivities, and their impact on ozone (O<sub>3</sub>) and secondary organic aerosol (SOA) formation throughout the year 2021. During the observation period, alkanes (40.13%) emerging as the predominant VOC species. Seasonal variation in VOCs followed the order of winter (26.49 ppb) > spring (23.63 ppb) > summer (23.62 ppb) > autumn (20.47 ppb). The results of positive matrix factorization (PMF) revealed that solvent usage, combustion, and vehicle exhaust were the dominant VOC sources. Regional transport from nearby provinces also significantly contributed to VOC levels. These contributions varied seasonally, with southeastern air masses prevailing in both spring and autumn, eastern air masses impacting summer, and northwestern air masses affecting winter. The campaign-averaged value of total hydroxyl (OH) radicals was 19.08 s<sup>-1</sup>. NO<sub>2</sub> accounted for the most significant contribution to the overall OH reactivity (39.11%), followed by VOCs (28.72%). Notable seasonal fluctuations in OH reactivity followed the order of winter (24.20 s<sup>-1</sup>) > spring (19.22 s<sup>-1</sup>) > autumn (18.07 s<sup>-1</sup>) > summer (14.86 s<sup>-1</sup>). The average ozone formation potential (OFP) for the measured VOCs was calculated as 75.54 ppb, with alkenes being the dominant contributor. The highest value was observed in spring (83.05 ppb), the lowest value was in autumn (60.43 ppb). The SOA formation potential, mainly contributed by the aromatics, was averaged as 2.92 μg m<sup>-3</sup>. Additionally, the top four SOA-contributing species across four seasons were toluene, benzene, *m*-xylene, and ethylbenzene. VOC-PM<sub>2.5</sub> sensitivity analysis showed that VOCs exhibited higher sensitivity to PM<sub>2.5</sub> on clean level (PM<sub>2.5</sub> < 35 μg m<sup>-3</sup>) than on level with heavy pollution. Alkenes, oxygenated volatile organic

compounds (OVOCs) and aromatics played significant roles in the transformations of O<sub>3</sub> and SOA in Hangzhou. Therefore, controlling the concentrations of these species is crucial for reducing complex atmospheric pollution in the region. Overall, this study compiles scientific evidence on pollution sources in Hangzhou, providing the government with valuable information.

#### KEYWORDS

volatile organic compounds, source appointment, ozone formation potential, SOA formations potential, atmospheric pollution

## 1 Introduction

In recent years, regions worldwide have been experiencing atmospheric pollution events, particularly severe haze episodes during winter and autumn and O<sub>3</sub> pollution in the summer (Zhang et al., 2018; Yadav et al., 2019; Uttamang et al., 2020; Yu et al., 2022). Volatile organic compounds (VOCs), which are common precursors of ozone (O<sub>3</sub>) and fine particulate matter (PM<sub>2.5</sub>), are considered significant pollutants contributing to regional atmospheric composite pollution in China. They are closely associated with atmospheric pollution events such as photochemical smog and haze, which can potentially harm human health. Consequently, they have become a global focus for air pollution prevention and control. Additionally, the mechanisms underlying the impact of VOCs on the environment are not yet fully understood. Therefore, the investigation of VOCs remains a central focus for both the scientific community and relevant regulatory authorities (Xu et al., 2017; Liu et al., 2019b; Song et al., 2019).

VOCs encompass a wide range of species, each with varying chemical reactivity. Thus, researchers have focused on elucidating VOC characteristics and identifying key active substances. Studies have often highlighted alkanes as the primary VOCs, while aromatics and alkenes are typically deemed more significant contributors to ozone formation potential (OFP). However, the influence of OVOCs has been overlooked (Guo et al., 2017; Han et al., 2023). Han et al. (2023) indicated that alkanes constituted the predominant group, comprising 60.88% of the total VOC concentration, while alkenes were the largest potential contributor to OFP. However, Louie et al. (2013) reported that OVOCs significantly contributed to OFP in the Greater Bay Area, accounting for more than one-third of the total impact of VOCs. This finding underscores the importance of OVOCs in OFP calculations and their subsequent impact on atmospheric chemistry. Additionally, OVOCs are recognized for their active participation in atmospheric photochemistry, leading to the formation of secondary gaseous and particulate products through chain reactions. Given the significant contribution of OVOCs to OFP, studying the impact of OVOCs is crucial. However, considering the complex composition of atmospheric VOCs, identifying their sources is challenging.

Field measurements revealed that fluctuations in atmospheric oxidation capacity (AOC) influenced O<sub>3</sub> levels and significantly affected the production of secondary particles year-round (Prinn, 2003). However, short-term monitoring data for VOCs, typically covering a few days to a couple of months, are more prevalent than data collected over extended periods (Mozaffar and Zhang, 2020; Yu

et al., 2022). This phenomenon hinders the development of a comprehensive understanding of VOC pollution. Moreover, previous studies have predominantly concentrated on variations in AOC, with a limited understanding of the seasonal variations of AOC produced by VOCs, which are expected to be significant. Thus, it is crucial to conduct long-term investigations and assess seasonal variations in AOC. VOCs are important precursors for the formation of secondary organic aerosols (SOAs) (Chen et al., 2011; Tong et al., 2013). Numerous studies have conducted chamber experiments (Pankow et al., 2001; Dechapanya et al., 2003; Chen et al., 2011) to delineate the properties of haze and calculate SOA yields from the precursors (Seinfeld et al., 2001; de Gouw et al., 2011; Gentner et al., 2017). Model predictions typically yield values that are underestimated compared with measured values in urban areas (Ait-Helal et al., 2014; Fu et al., 2014; Han et al., 2017). Furthermore, there is limited understanding regarding the qualitative and quantitative differences between VOCs and PM<sub>2.5</sub> (Yamada, 2013; Mo et al., 2015; Han et al., 2017). Hence, investigating the combined effects of the physical evolution and chemical reactions of VOCs on SOA formation is crucial.

Hangzhou, the political and cultural hub of Zhejiang Province, spans an expansive 16,850 square kilometers and has a population exceeding 12 million. This region has frequently suffered from severe haze episodes and photochemical pollution, primarily stemming from the substantial release of air pollutants, as documented in the Environmental and Ecological Status Bulletins in China (<http://www.mee.gov.cn/hjzl/>). Extensive studies have been conducted on air pollution in Hangzhou, with many of the earlier studies focusing on VOC concentrations (Wang et al., 2019). However, there remains limited understanding from previous research regarding the formation of O<sub>3</sub> and SOA from VOCs, as well as the relationships between VOCs, PM<sub>2.5</sub>, and O<sub>3</sub>, particularly concerning long-term and seasonal variations (Ying et al., 2012; Jing et al., 2020a). Following policy adjustments and improvements to the energy infrastructure, recent mitigation efforts may have altered the characteristics of VOCs. Therefore, it is crucial to examine the specific features of local VOC pollution using an extended time series of monitoring data. This information can provide valuable insights for shaping local air pollution control strategies.

To further elucidate the characteristics of VOC pollution, source contributions, and secondary formations of O<sub>3</sub> and SOA, high-temporal-resolution measurements of VOCs were conducted in Hangzhou from January 1st to 31 December 2019. The objectives of this research are to 1) analyze the characteristics and seasonal variations in VOCs, 2) identify the contributions of VOC sources, 3) speciate OH reactivity among seasonal variations, and 4) quantitatively assess the contributions of VOCs to the formation of PM<sub>2.5</sub> and O<sub>3</sub>.

## 2 Observation and methods

### 2.1 Site description

The site of Zhuantang (ZT) (30.15°N, 120.08°E) is situated southwest upwind of the urban area. There are no discernible pollution sources nearby, and the observation period spans throughout 2021 (Supplementary Figure S1). Elevated roads and the Hangzhou Bypass Road are nearby, while the Changshen Highway is 500 m away. To the north of this observation point lies the West Lake Scenic Area. Parks, such as Xinshixun Science and Technology Park or Liouliang Industrial Village, are located 12–20 km away in the northwest. In the northeastern direction, Nanshingqiao Freight Railway Station, Hangzhou Station, and Hangzhou East Station are located about 20 km away. Furthermore, approximately 20 km to the southwest are industrial estates such as Jinqiao Industrial Park or Chunjian Industrial Park. In summary, the site of ZT in Hangzhou's Xihu District, constitutes a typical urban integrated functional area. Additionally, it reflects the regional characteristics of urban air pollution in Hangzhou to a certain extent.

### 2.2 Sampling and chemical analysis

VOCs (29 alkanes, 11 alkenes, 1 alkyne, 17 aromatics, and 20 OVOCs) were sampled at an interval of 6 days and sampling began at 10:00 a.m. on each sampling days and ended at 10:00 a.m. on the next day using a 3.2 L SUMMA passivated stainless steel tank (ENTECH Instruments, Inc., United States) combined with ENTECH 1900 (ENTECH Instruments, Inc., United States) handheld injector and an MH1200-B automatic atmospheric sampler (Minhope Instruments Inc., Qingdao, China), which was employed for constant flow sampling lasting 24 h. The samples were then analyzed using a Superlab 2020-TT-GCMS (Panhe Scientific Instrument Co., Ltd., Shanghai, China) SUMMA tank automatic constant-flow sampling system. Ethane, ethylene, acetylene, propane, and propene were identified using an FID detector, while the remaining VOC compounds were detected using an MS detector. A PLOT column (Al/KCl, 30 m × 0.25 mm × 5 μm) was used as the FID chromatographic column, and a BD-624 column (60 m × 0.25 mm × 1.4 μm) was utilized as the MS chromatographic column. The MS column was analyzed using the full-scan depth mode (Jing et al., 2020b).

The concentrations of major pollutants such as PM<sub>2.5</sub>, CO, SO<sub>2</sub>, O<sub>3</sub>, and NO<sub>x</sub> were measured using the following instruments: PM<sub>2.5</sub> levels were continuously monitored using a Thermo Scientific™ Model 5030i SHARP particulate matter monitor. CO concentrations were measured using a Thermo Scientific™ Model 48i analyzer, which is equipped with gas filters and NDIR technology to ensure accurate and reliable readings. To ensure excellent detection specificity and long-term stability in measuring SO<sub>2</sub>, the Thermo Scientific™ SO<sub>2</sub> analyzer utilizes a pulsed fluorescence technique. O<sub>3</sub> was measured using the Thermo Scientific™ 49i dual-chamber ultraviolet photometric ozone analyzer. For measuring NO<sub>x</sub> concentrations, the Thermo Scientific™ Model 42i analyzer, which employs chemiluminescence, was utilized, allowing for independent calibration. Each of the trace gas analyzers was

checked every day for zero calibration, along with weekly calibration and monthly multipoint calibration. Meteorological data, including temperature, relative humidity (RH), and wind speed, were obtained from each meteorological station.

### 2.3 Methods

#### 2.3.1 Positive matrix factorization model

The positive matrix factorization (PMF) model is a source–receptor statistical factor analysis method widely used for apportioning sources of air pollution. In the current study, the U.S. EPA PMF 5.0 receptor model was employed for the source apportionment of measured VOC species. The method is detailed in Paatero and Tapper (1994). The monitoring data samples can be represented as a matrix  $X$  with  $i$  rows and  $j$  columns, where  $i$  represents the number of samples, and  $j$  represents the number of measured species. Any matrix  $X$  can be decomposed into a factorial product of two matrices: the factor contribution matrix  $g$  ( $i \times p$ ) and the factor profile matrix  $f$  ( $p \times j$ ), along with a residual part not explained by the model,  $e$ . The mass of each measurement sample is calculated according to Eq. 1, where the number of source factors is  $p$ .

$$X_{ij} = \sum_{k=1}^p g_{ik} f_{kj} + e_{ij} \quad (1)$$

According to the  $Q_{\text{true}}/Q_{\text{robust}}$  value, choosing an optimal number of factors in a model is essential.  $Q_{\text{true}}$  is the actual value calculated using the PMF model, while  $Q_{\text{robust}}$  is the value calculated after correcting for missing values or outliers (Brown et al., 2015). Theoretically, the analysis is considered reasonable when  $Q_{\text{true}}/Q_{\text{robust}} < 1.5$  and tends to be 1. The objective function  $Q$  is shown in Eq. 2, where  $u_{ij}$  represents the uncertainty associated with  $X_{ij}$ .

$$Q = \sum_{i=1}^n \sum_{j=1}^m \left[ \frac{x_{ij} - \sum_{k=1}^p g_{ik} f_{kj}}{u_{ij}} \right]^2 \quad (2)$$

Two input files are required by the PMF: one for concentration values and another for uncertainty values for individual VOC species. The data's uncertainty ( $Unc$ ) is determined by the method detection limit (MDL) and the error fraction (EF) of the measurement, as presented in Eq. 3.

$$Unc = \begin{cases} \sqrt{(ErrorFraction \times Conc.)^2 + (0.5 \times MDL)^2} & Conc. > MDL \\ \frac{5}{6} \times MDL & Conc. \leq MDL \end{cases} \quad (3)$$

The EF can be set to 5%–20% when the concentration of the measured data is higher than the MDL (Song et al., 2007; Hui et al., 2018). In this study, the EF was set to 10%. Data below the detection limit were replaced with 1/2 MDL, corresponding to an uncertainty of 5/6 MDL.

#### 2.3.2 Backward trajectory analysis

Trajectory clustering analysis is a clustering method based on the trajectory data of moving objects. The main aim of the study is to summarize and categorize an extensive collection of data on trajectory, which share similar movement characteristics with

research subjects. In this study, an Eulerian distance estimation algorithm is used to calculate the relevant trajectories based on air mass velocity. To avoid ground friction interference with air mass trajectories, the study employs MeteInfoMap software, which provides trajectory analysis at a near-surface height of 500 m. A 24-h calculation period is used to analyze air mass trajectory and sources in Hangzhou during the year 2021. The hourly meteorological data were obtained from the Global Data Assimilation System provided by the National Oceanic and Atmospheric Administration (NOAA., <ftp://arlftp.arlhq.noaa.gov/pub/archives/gdas1>).

### 2.3.3 OH reactivity

Thousands of trace gases released into the atmosphere will eventually chemically react with hydroxyl radicals. OH is primarily produced by the photolysis of O<sub>3</sub> and by the reaction of excited-state atomic oxygen with water vapor. The total OH reactivity is defined as the combined effect of all OH reactants on the frequency of instantaneous OH loss in the atmosphere (s<sup>-1</sup>), which is essentially the inverse of the OH chemical lifetime. The OH reactivity, as calculated using Eq. 4 in this study, depends on the concentrations of all OH-reactive trace gases and their reaction rate coefficients with OH. These factors collectively determine the inverse of the OH chemical lifetime, influencing the abundance of OH and the efficiency in the atmosphere cleaning process. Continued OH production results in a decrease in overall OH concentrations in the atmosphere as OH reactivity increases. Additionally, the chemical activity of VOCs in the air varies widely and exerts various impacts on atmospheric reactivity.

$$\begin{aligned} \text{Total OH reactivity} = & \Sigma k_{\text{OH}+\text{VOC}_i} [\text{VOC}_i] + \Sigma k_{\text{OH}+\text{CO}} [\text{CO}] \\ & + \Sigma k_{\text{OH}+\text{NO}} [\text{NO}] + \\ & \Sigma k_{\text{OH}+\text{NO}_2} [\text{NO}_2] + \Sigma k_{\text{OH}+\text{SO}_2} [\text{SO}_2] + \Sigma k_{\text{OH}+\text{O}_3} [\text{O}_3] \end{aligned} \quad (4)$$

where  $k_{\text{OH}+\text{VOC}_i}$ ,  $k_{\text{OH}+\text{CO}}$ ,  $k_{\text{OH}+\text{NO}}$ ,  $k_{\text{OH}+\text{NO}_2}$ ,  $k_{\text{OH}+\text{SO}_2}$ , and  $k_{\text{OH}+\text{O}_3}$  denote the reaction constants (cm<sup>3</sup> molecule<sup>-1</sup> s<sup>-1</sup>) of the VOC species, CO, NO, NO<sub>2</sub>, SO<sub>2</sub>, and O<sub>3</sub>, respectively, with OH radicals. These values were sourced from Atkinson and Arey (2003). [VOC<sub>*i*</sub>], [CO], [NO], [NO<sub>2</sub>], [SO<sub>2</sub>], and [O<sub>3</sub>] denote the concentrations of the VOC species, CO, NO, NO<sub>2</sub>, SO<sub>2</sub>, and O<sub>3</sub>, respectively (molecule cm<sup>-3</sup>).

### 2.3.4 OFP

The methodology employed in this paper is based on Carter's maximum incremental reactivity (MIR) method for evaluating the OFP of VOCs (Carter, 1994; 1997) (Supplementary Table S1). MIR is commonly employed to gauge the chemical reactivity of different VOCs, while OFP is used to measure the impact of various VOCs on O<sub>3</sub> formation. The OFP values of different VOC species can be determined using Eq. 5:

$$\text{OFP}_i = [\text{VOCs}]_i \times \text{MIR}_i \quad (5)$$

### 2.3.5 SOA formation potential

SOA is a significant atmospheric pollutant involved in haze formation. It is primarily produced through the oxidation and air-particle partitioning of both natural and anthropogenic VOC emissions. In this study, the potential of VOCs to form SOA is

investigated using the secondary organic aerosol potential (SOAP) parameter developed by Derwent et al. (2010) (Supplementary Table S1). SOAP is typically denoted by a toluene index of 100 and is calculated by summing the SOAP values of all VOC species, as illustrated in Eq. 6. Here, VOC<sub>*i*</sub> represents the concentration of the measured species *i*, and SOAP<sub>*i*</sub> denotes the SOAP value of the measured species *i*.

$$\text{SOAP} = [\text{VOCs}]_i \times \text{SOAP}_i \quad (6)$$

### 2.3.6 VOC-PM<sub>2.5</sub> sensitivity analysis

Previous studies have shown that a qualitative description of VOC and PM<sub>2.5</sub> evolution can be obtained at every concentration interval. However, it remains challenging to conduct a quantitative analysis of the evolution patterns of VOCs and PM<sub>2.5</sub>. To assess the impact of PM<sub>2.5</sub> concentration on VOCs, Han et al. formulated equations (Eqs. 7; 8) for sensitivity coefficients, enabling a more precise determination of their correlation (Han et al., 2017; Han et al., 2018a).

$$\eta = \frac{\Delta_{\text{VOCs}}}{\Delta_{\text{PM}_{2.5}}} \quad (7)$$

$$\text{VOCs} - \text{S} = \frac{\eta_{\Delta}}{\eta_{\text{B}}} = \frac{\Delta_{\text{VOCs}}/\text{B}_{\text{VOCs}}}{\frac{\Delta_{\text{PM}_{2.5}}}{\text{B}_{\text{PM}_{2.5}}}} \quad (8)$$

where Δ<sub>VOCs</sub> and Δ<sub>PM<sub>2.5</sub></sub> characterize the concentrations of VOCs and PM<sub>2.5</sub> (μg m<sup>-3</sup>) under the specified PM<sub>2.5</sub> concentration range, and B<sub>VOCs</sub> and B<sub>PM<sub>2.5</sub></sub> represent the background concentrations of VOCs and PM<sub>2.5</sub>, respectively.

In this study, PM<sub>2.5</sub> concentrations averaging <20 μg m<sup>-3</sup> are labeled B<sub>PM<sub>2.5</sub></sub>, while the corresponding average VOC concentrations are denoted as B<sub>VOCs</sub> (Han et al., 2017; Han et al., 2018a). Generally, a higher value of the VOC-S coefficient suggests greater sensitivity of VOC concentration to changes in PM<sub>2.5</sub> concentration. This implies that VOC concentration fluctuates more while the PM<sub>2.5</sub> concentration changes less.

## 3 Results and discussion

### 3.1 Characteristics of VOCs

#### 3.1.1 Concentrations and compositions of VOCs

The time series of meteorological factors, VOCs, NO<sub>x</sub>, SO<sub>2</sub>, CO, O<sub>3</sub>, and PM<sub>2.5</sub> at the ZT site are depicted in Figure 1. The average temperature was 17.19°C ± 8.59°C, and the mean RH was 81.31% ± 12.43%. The wind speed ranged from 0.48 to 5.18 m s<sup>-1</sup>, with a mean value of 1.18 ± 0.63 m s<sup>-1</sup>. The mean concentrations of SO<sub>2</sub> and CO were 4.21 ± 1.02 μg m<sup>-3</sup> and 0.64 ± 0.17 mg m<sup>-3</sup>, with ranges of 1.02–9.83 μg m<sup>-3</sup> and 0.16–1.30 mg m<sup>-3</sup>, respectively. The mean concentration of NO<sub>x</sub> was 33.47 ± 14.39 μg m<sup>-3</sup>. These results were comparable to those observed in Hangzhou and Shanghai, China (Mao et al., 2022; Han et al., 2023).

The campaign-averaged maximum and minimum concentrations were respectively obtained as 3 and 173.5 μg m<sup>-3</sup> for PM<sub>2.5</sub> and 2.33 and 145 μg m<sup>-3</sup> for O<sub>3</sub>, with the average concentrations of 34.15 ± 21.35 μg m<sup>-3</sup> and 33.67 ± 19.68 μg m<sup>-3</sup> for PM<sub>2.5</sub> and O<sub>3</sub>, respectively. Generally, the concentration of PM<sub>2.5</sub>

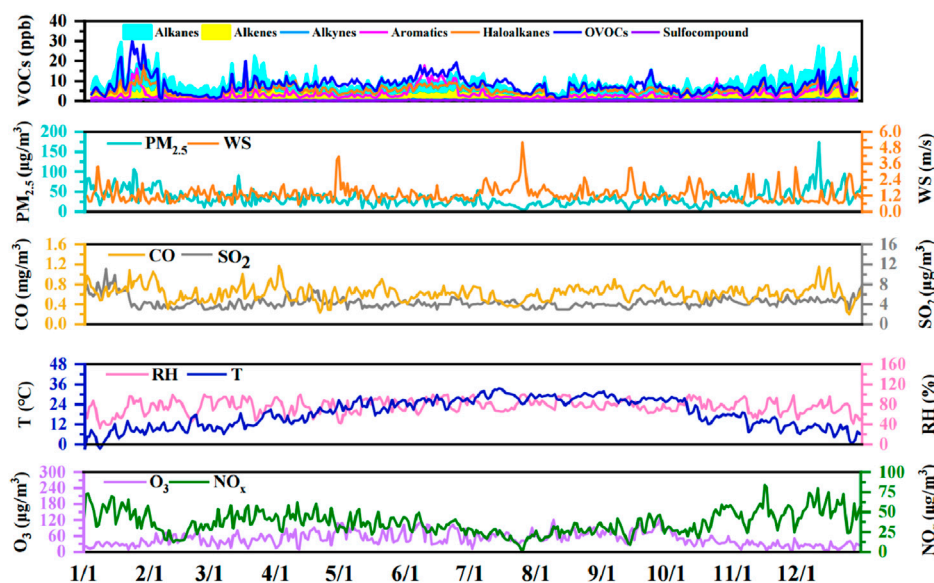


FIGURE 1 Time series of VOCs,  $PM_{2.5}$ , CO,  $SO_2$ ,  $O_3$ ,  $NO_x$ , and meteorological parameters (temperature [T], relative humidity [RH], and wind speed [WS]) during the observation period.

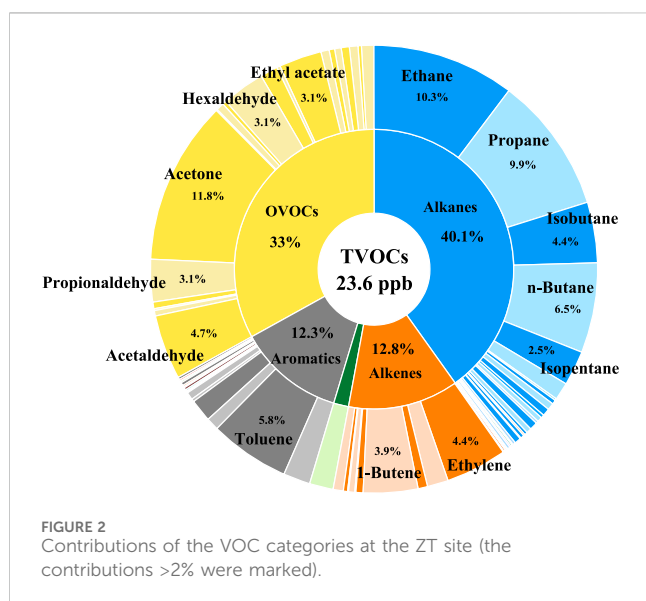


FIGURE 2 Contributions of the VOC categories at the ZT site (the contributions >2% were marked).

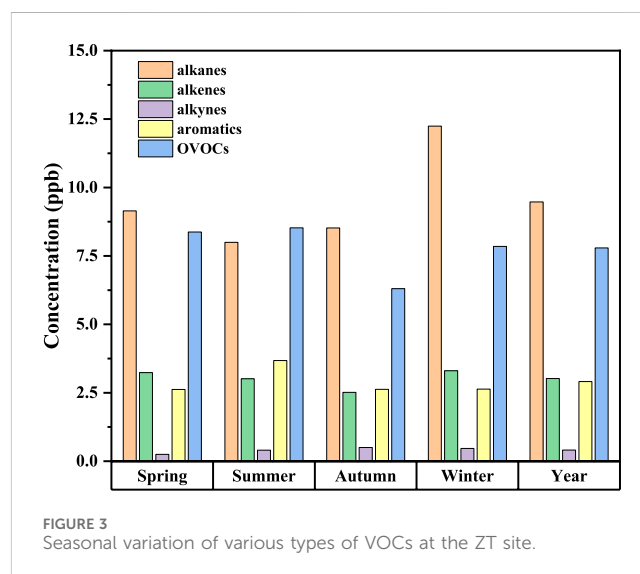
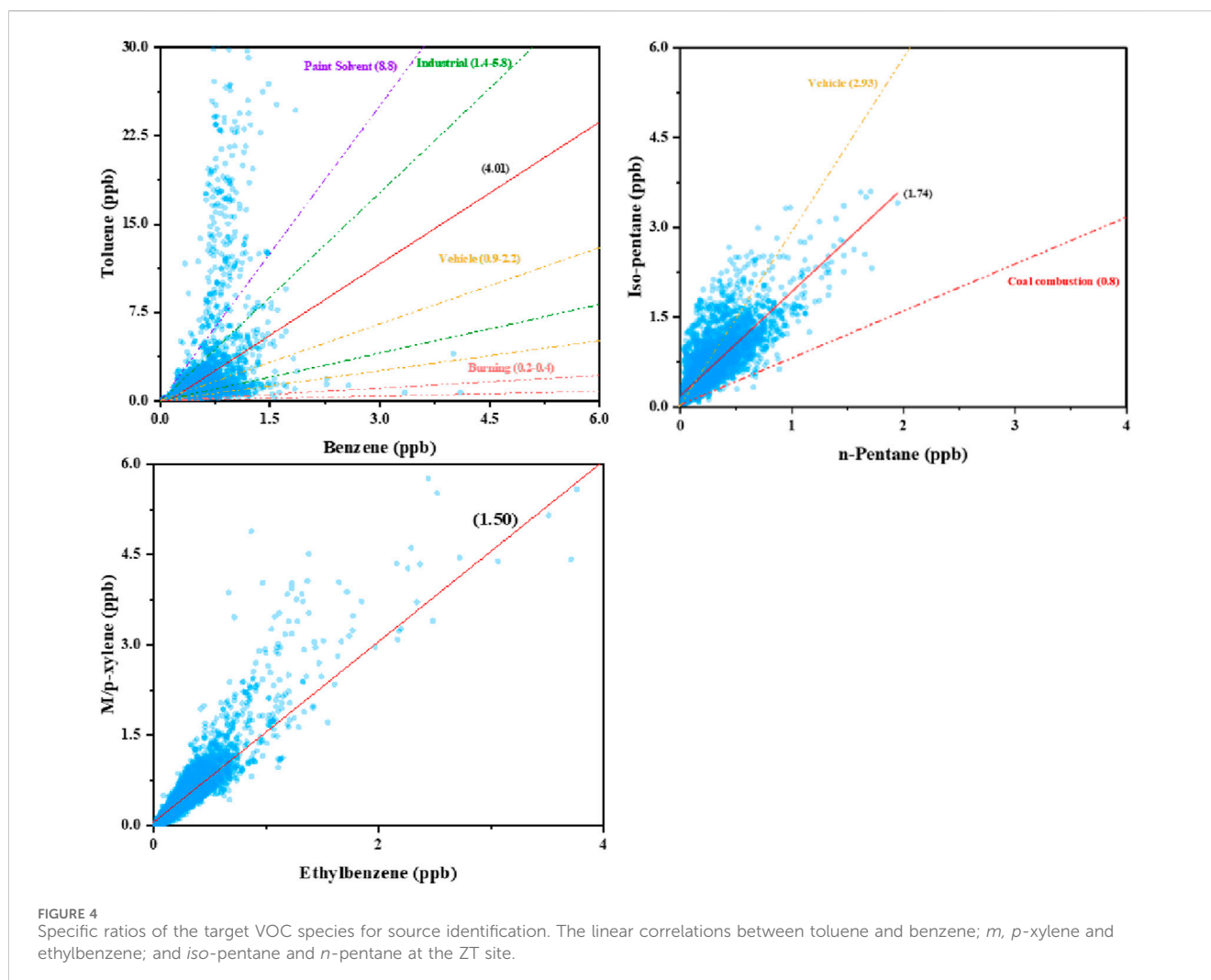


FIGURE 3 Seasonal variation of various types of VOCs at the ZT site.

was lower than those recorded in December 2017, where the  $PM_{2.5}$  concentration was  $52.4 \mu\text{g m}^{-3}$  in urban Shanghai (Liu et al., 2021a). The average  $O_3$  concentration was considerably lower than those obtained for Xi'an, China ( $102 \mu\text{g m}^{-3}$ ) (Song et al., 2021); Beijing-Tianjin-Hebei, China ( $154 \mu\text{g m}^{-3}$ ) (Yang et al., 2020); Hamburg, Germany ( $120.6 \mu\text{g m}^{-3}$ ) (Krug et al., 2020); and Leipzig, Germany ( $139.9 \mu\text{g m}^{-3}$ ) (Krug et al., 2020). As a crucial precursor of  $O_3$ , the trend observed in VOC concentration exhibited an inverse correlation with that of  $O_3$ . Specifically, when atmospheric VOCs accumulate to a particular threshold level, there is a gradual increase in  $O_3$  concentration via photochemical reactions, coinciding with a decrease in VOC concentration (Song et al., 2018; Yang et al., 2020).

During the whole year of 2021, the average VOC concentration was 23.60 ppb (Figure 2), comparable to the concentration of VOCs in Shanghai, China (21.36 ppb) (Han et al., 2023), but lower than those in Hangzhou, China (32.00 ppb) (Han et al., 2019), Guangzhou, China (42.7 ppb) (Zou et al., 2015), 3China (34.4 ppb) (Shao et al., 2016), Beijing, China (53.5 ppb) (Liu et al., 2020), Tianjin ( $30.6 \pm 24.0$  ppb) (Gu et al., 2020) and Delhi, India (54.59 ppb) (Kumar et al., 2018). Compared with the relevant observation performed previously in Hangzhou, this study generally presented lower VOC concentrations (Han et al., 2019; Li et al., 2023). The major VOC component was alkanes, with an average concentration of 9.47 ppb, comprising 40.13% of the total VOC (TVOC) concentration, followed by OVOCs (7.79 ppb,



33.02%), alkenes (3.02 ppb, 12.80%), aromatics (2.91 ppb, 12.33%), and alkyne (0.41 ppb, 1.72%). The significant contribution of alkanes is attributable to their extensive emission sources and prolonged atmospheric lifetimes.

### 3.1.2 Seasonal variations

The VOC concentrations exhibited significant seasonal variations (Figure 3; Supplementary Figure S2). The TVOC concentrations declined in the order of winter (26.49 ppb) > spring (23.63 ppb) > summer (23.62 ppb) > autumn (20.47 ppb). Similar seasonal trends were observed for the majority of VOC components, except for OVOCs.

Seasonal fluctuations in OH radicals, the distribution and intensity of emission sources, and meteorological conditions significantly contributed to notable variations in the observed levels of VOCs. The heightened dispersion and convection of pollutants, driven by deep mixing during summer and autumn, contributed to the reduction of VOCs (Modon et al., 2001; Kumar et al., 2018). Additionally, elevated temperatures and increased solar radiation can lead to greater VOC losses through photochemical degradation during the summer, resulting in the formation of simpler molecules such as CO, CO<sub>2</sub>, and other intermediates (Lai et al., 2013). The presence of increased atmospheric stability and

calm conditions restricted the dispersion of pollutants, consequently leading to higher levels of VOCs during the winter season (Dumanglu et al., 2014). Apart from those, photochemical reactivity was also an important factor leading to higher levels of VOCs that cannot be ignored. OVOCs are primarily generated via the oxidation of biogenic and anthropogenic hydrocarbons and other organic compounds in the atmosphere (Finlayson-Pitts and Pitts, 2000), with additional emissions from vegetation. Therefore, the seasonal variation of OVOCs followed the order: summer > spring > winter > autumn, consistent with the findings of Gu et al. (2019).

## 3.2 Source apportionment

### 3.2.1 Special VOC ratio analysis

Various types of VOC species originate from distinct sources, and analyzing the ratio of these different species could serve as a preliminary method for distinguishing emission sources (An et al., 2014). In this study, we employed variations in the ratios of toluene/benzene (T/B), *iso*-pentane/*n*-pentane (P/P), and *m*, *p*-xylene/ethylbenzene (X/E) at the sampling sites to identify the sources of VOC emissions. The results are presented in Figure 4.

Diverse VOC sources can be identified according to distinct T/B ratios (Song et al., 2021). The mean T/B ratio was  $4.01 \pm 0.11$ , with Pearson correlation coefficients ( $R_{Pearson}$ ) of 0.38. Most of the ratios (44.58% and 49.69%) fall within the ranges of 0.9–2.2 and 1.4–5.8, indicating significant impacts of vehicular emissions and industrial emissions on VOC concentrations, consistent with previous studies (Zhang et al., 2013; Shi et al., 2015; Yao et al., 2015; Deng et al., 2018; Han et al., 2023). This observation is attributable to the distribution of industrial enterprises such as Jinqiao Industrial Park and Chunjian Industrial Zone, which are located 20 km away from the sampling site in the southwest direction. Additionally, Hangzhou, as a transportation hub, hosts a substantial fleet of motor vehicles, necessitating the reinforcement of regional measures to control motor vehicle usage.

The sources originating from fossil fuels (vehicle exhaust, fuel evaporation, and coal combustion) can be further distinguished according to the P/P ratio. *Iso*-pentane and *n*-pentane, having similar atmospheric lifetimes, exhibited similar trends and demonstrated a high correlation ( $R_{Pearson} = 0.81$ ), therefore featuring similar sources of emissions (Jobson et al., 1998; Yan et al., 2017). Different emission sources are distinguished by specific VOC species. Lower P/P ratios (0.56–0.80) are typically associated with coal combustion (Li et al., 2019a; Han et al., 2023), while P/P ratios in the range of 2.2–3.8 are indicative of vehicular emissions (Wang et al., 2013; Han et al., 2023). After linear straight fitting and correction, the mean P/P ratio was determined as  $1.74 \pm 0.02$ , indicating that both vehicular emissions and coal combustion were critical factors influencing the concentration of VOCs at the ZT site.

In addition to local emissions affecting VOC pollution characteristics, regional transport has been investigated as a potential source of VOCs (Nelson and Quigley, 1983; Chang et al., 2006; Vardoulakis et al., 2011). In this study, we utilized the X/E ratio to assess the influence of transport. *m*, *p*-xylene, and ethylbenzene have been observed to share similarities in emission sources, with the former demonstrating approximately three times greater reactivity toward the OH radical compared with the latter (Chang et al., 2006; Vardoulakis et al., 2011). Therefore, lower X/E ratios typically indicate more pronounced air mass aging, signifying a greater influence from external transport. The average X/E ratio was  $1.50 \pm 0.01$ , indicating significant external transport at the sampling site.

### 3.2.2 PMF analysis

PMF analysis enables the quantitative assessment of VOC sources (Hui et al., 2019; Han et al., 2023). In this study, the PMF model incorporated 34 VOC species, leading to the identification of five distinct factors contributing to VOC emissions: solvent usage, vehicle exhaust, industrial sources, combustion, and biogenic sources. The source profiles of these factors as resolved by the PMF model are illustrated in Figure 5.

Solvent usage can be identified by the presence of certain alkanes and aromatics, such as benzene, toluene, ethylbenzene, and xylene (Wang et al., 2013; Hui et al., 2018; Song et al., 2019a). In the present study, high contributions to VOC emissions were observed from toluene (55.80%), ethylbenzene (64.11%), *o*-xylene (66.41%), *m*/*p*-xylene (71.13%), and styrene (45.61%). Emission factors meeting these characteristics were identified, and paint solvent usage

accounted for 24.10% of the total VOC emissions. These significant findings suggest that solvent usage was the predominant source of VOCs at the ZT site.

Vehicle exhaust emissions are characterized by high percentages of alkanes, some alkenes, and aromatics (Ling et al., 2011; An et al., 2017; Hui et al., 2018). In this study, high proportions of ethane (46.59%), *n*-pentane (40.96%), *n*-hexane (43.01%), cyclohexane (49.64%), ethylene (36.27%), acetylene (39.85%), benzene (30.66%), ethylbenzene (25.26%), and *m*/*p*-xylene (29.79%) were observed. These compounds are commonly recognized as tracers for vehicular emissions (An et al., 2017; Hui et al., 2018). In this study, PMF analysis revealed that vehicle exhaust sources ranked as the third-largest source of VOCs, accounting for 19.75% of the VOCs at the sampling site. The consistently high results suggest that vehicle exhaust was one of the primary sources of VOCs, aligning with the abovementioned P/P ratio findings. Vehicle exhaust has been established as one of the primary contributors to local air pollution in Hangzhou (Jing et al., 2020a).

Industrial sources are characterized by high proportions of aromatics and certain proportions of alkanes, as noted in previous studies (Guo et al., 2011; Sun et al., 2016). In this study, significant contributions to VOC emissions were observed from toluene (43.11%), benzene (38.35%), 2-methylhexane (35.64%), and 3-methylhexane (47.90%). Aromatic compounds are widely utilized in industrial solvent usage and manufacturing processes (Morrow, 1990; Ling et al., 2011). Therefore, industrial sources contributed to VOC emissions at the sampling site. Industrial activities accounted for 17.22% of the VOC emissions.

Combustion factor was characterized by  $C_2$ – $C_3$  alkanes such as ethane and propane;  $C_2$ – $C_3$  alkenes such as ethene and propene; acetylene; and certain aromatics such as benzene, toluene, and ethylbenzene (Liu et al., 2008; Ling et al., 2011; Song et al., 2018). Furthermore, the proportions of propene, *n*-hexane, *n*-heptane, and toluene in previous studies were relatively small, but the impacts of compounds warrant investigation (Hui et al., 2018; Han et al., 2023). High contributions to VOC emissions were observed for ethane (34.40%), propane (55.81%), ethylene (27.37%), propylene (41.26%), and acetylene (21.12%), highlighting the combustion source. In this study, combustion accounted for 22.74% of VOCs at the sampling site, indicating a significant impact of combustion, following the solvent-related source mentioned earlier.

Biogenic sources can be identified by the presence of isoprene (Ling and Guo, 2014; Ling et al., 2019; Song et al., 2021). Isoprene significantly contributed to VOC emissions, constituting 79.68% of the total VOCs at the sampling site, acting as a tracer released from biogenic sources (Kumar et al., 2018). Emissions from biogenic sources were estimated to contribute 16.18% to the total VOCs detected.

According to the PMF analysis results from the ZT site, the primary sources of VOCs are solvent usage, combustion sources, and vehicular emissions. These findings were similar to those of a study conducted in Hangzhou in 2021 (Li et al., 2023). In terms of VOC components, the proportion of aromatics at the ZT site in Hangzhou (12.3%) exceeded those in Beijing (9.9%) and Wuhan (11.9%) (Gao et al., 2021). This suggests that solvent usage was a more significant source in the suburban areas of Hangzhou, which aligns with the actual situation of heavy solvent usage (such as

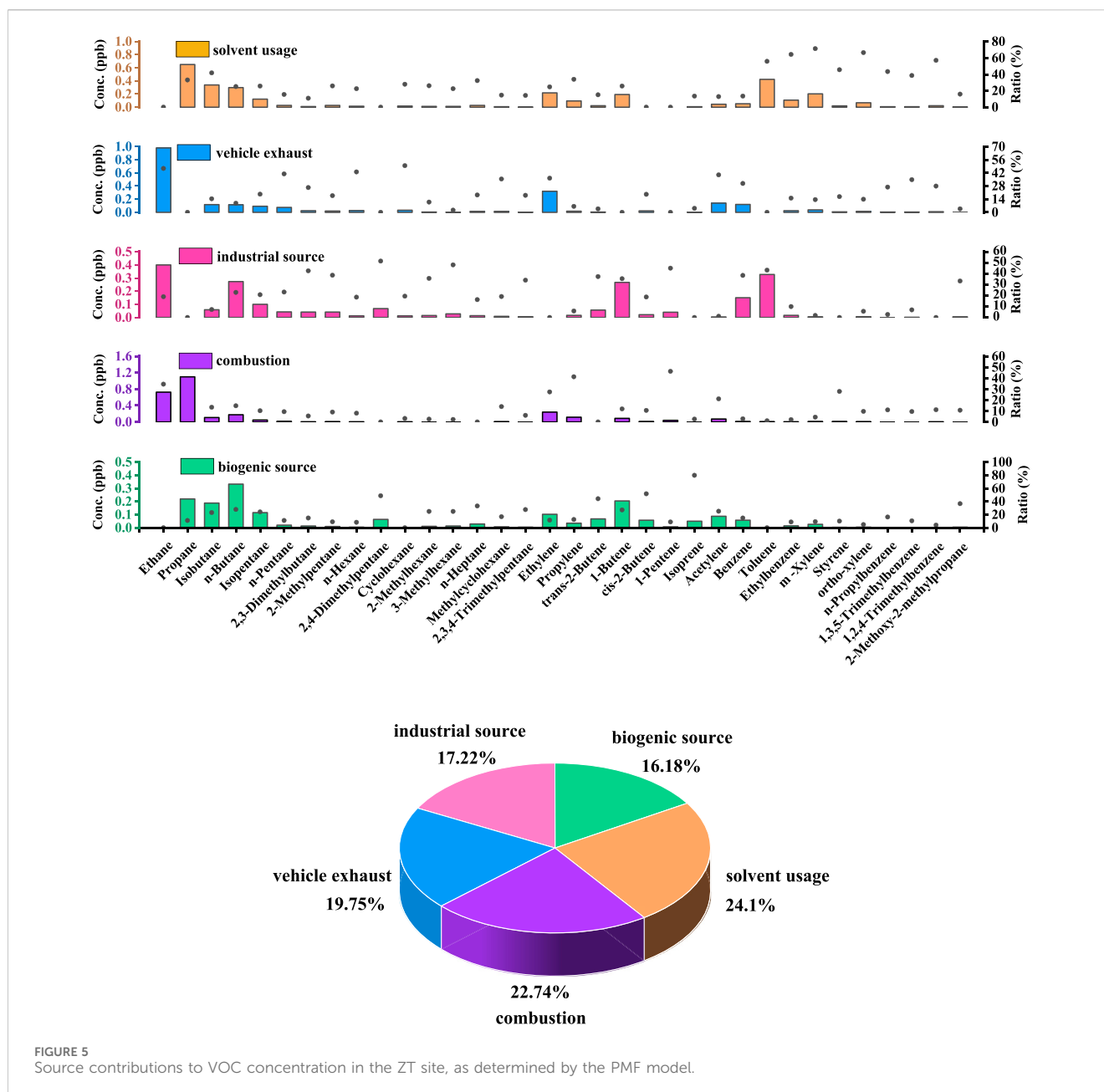


FIGURE 5 Source contributions to VOC concentration in the ZT site, as determined by the PMF model.

adhesives, coatings, and paints) in the manufacturing industry in East China (Gao et al., 2021). The high proportion of combustion sources is attributable to local fuel combustion in Hangzhou, including natural gas and coal. Additionally, combustion processes are prevalent in the daily lives of residents and commercial settings, such as the use of gas stoves and heating equipment in households and the use of boilers for commercial purposes. As of the end of 2022, the number of motor vehicles in Hangzhou has exceeded 4 million, indicating the significant impact of vehicle exhaust on VOCs in the city. This finding aligns well with those of other studies conducted in Hangzhou (21.2%) (Jing et al., 2020b) and Nanjing (18%) (Xia et al., 2014). Therefore, controlling solvent usage, anthropogenic combustion sources, and vehicle exhaust emissions could be effective strategies for reducing VOCs in the Hangzhou region.

### 3.2.3 Back trajectories analysis

In addition to the direct impact of local sources, regional transport can also contribute to VOC pollution (Hui et al., 2018). To further identify the influence of long-distance transport sources, the backward trajectories during the observation period are presented in Figure 6. This figure illustrates the 24-h back trajectories of air masses originating at 500 m altitude, and five clusters were obtained through the clustering algorithm for all seasons. Overall, the trajectory direction and movement characteristics of air masses varied significantly by season, reflecting the seasonal changes in atmospheric circulation (Zhu et al., 2017). In spring, the top three transported air masses were the medium-distance air mass from the East China Sea (29.85%), the medium-distance air mass from southern Anhui Province (25.86%), and the near-distance air

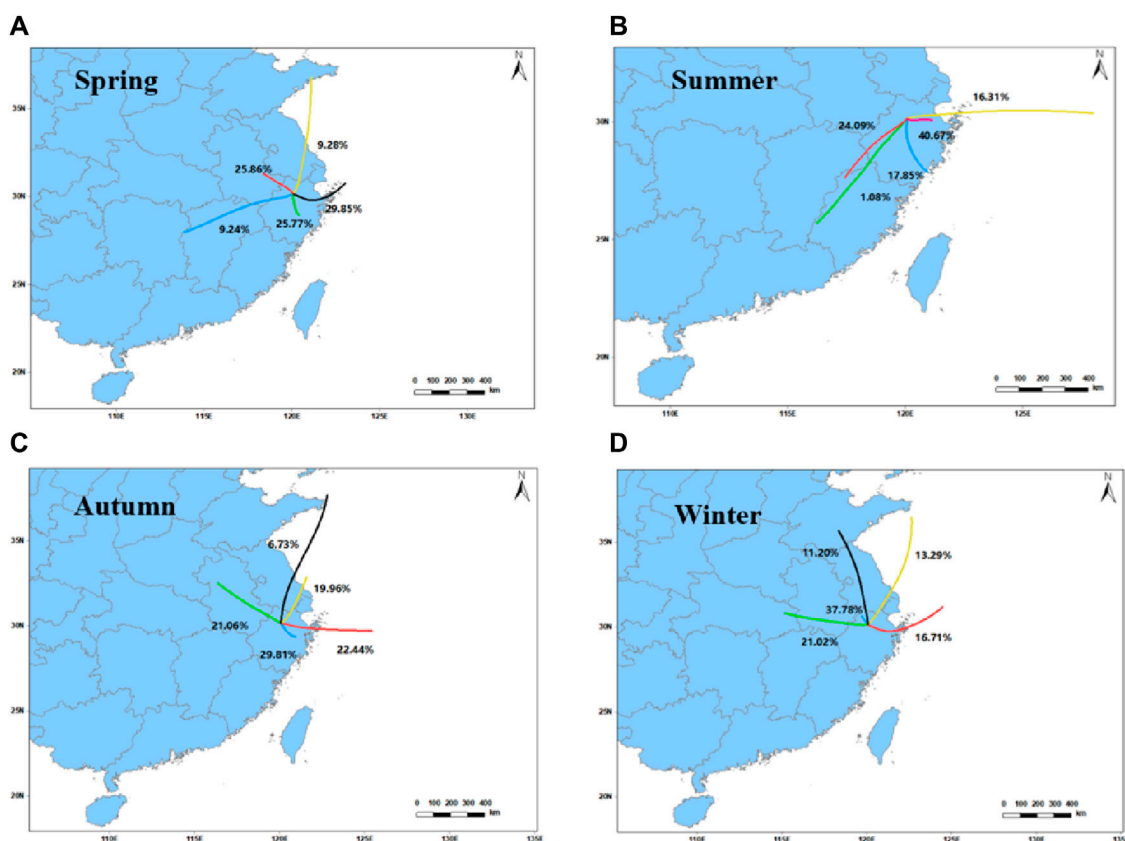


FIGURE 6 24-h daily mean backward trajectory clusters for (A) spring, (B) summer, (C) autumn, and (D) winter.

mass from southern Zhejiang Province (25.77%). The results indicated that the site was significantly affected by the southeast trajectory in spring. In summer, there were five clusters of trajectories observed at the site: eastern trajectories (Clusters 1 + 2), southern trajectories (Cluster 3), and southwestern trajectories (Clusters 4 + 5). The total contributions of eastern trajectories to the overall trajectory (56.98%) were significantly higher than those of the other two cluster trajectories. The eastern long-distance trajectory (Cluster 1) and the eastern short-distance trajectory (Cluster 2) accounted for 16.31% and 40.97% of VOC transportation. The southwestern long-distance trajectory (Cluster 4) and medium-distance trajectory (Cluster 5), categorized as the southwestern direction cluster, accounted for 1.08% and 24.09% of VOC transportation, respectively. The results indicated that VOC concentrations were significantly influenced by trajectories originating from the junction of eastern Zhejiang Province and Fujian Province, in addition to local emissions. In autumn, the majority of backward trajectories (52.25%) in Hangzhou originated from southeastern air masses, including those from the southern part of Zhejiang Province and mid-range air masses from the East China Sea (29.81% and 22.44%, respectively). This suggests that air masses from the southeastern direction had the greatest impact on Hangzhou during autumn. During winter, the most significant backward trajectories originated from the north of Hangzhou, accounting for 37.78%, followed by trajectories from the southeast of Hubei

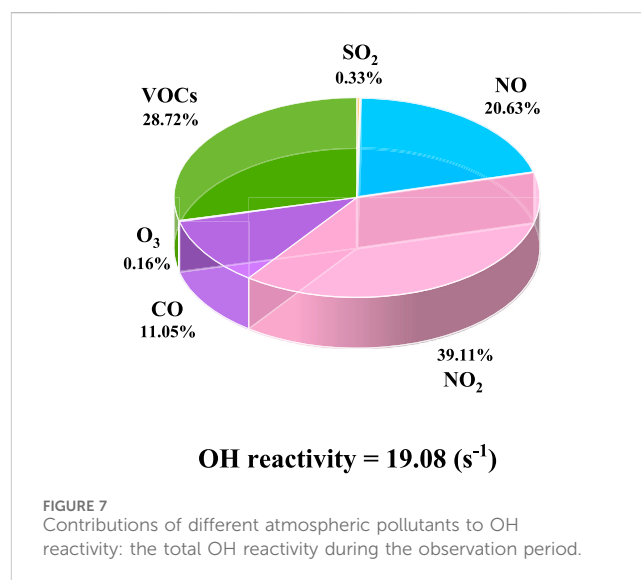


FIGURE 7 Contributions of different atmospheric pollutants to OH reactivity: the total OH reactivity during the observation period.

via Anhui, which accounted for 21.02%. In winter, the air masses affecting Hangzhou mainly originated from the north, southeast of Hubei province, and southeast of Shandong province, all originating from the northwest, with a combined contribution of 70.00%. This combination serves as the primary factor influencing atmospheric VOCs in Hangzhou during winter.

### 3.3 Atmospheric environmental implication

#### 3.3.1 OH reactivity

The calculated OH reactivity of trace gases was categorized into  $\text{SO}_2$ , NO,  $\text{NO}_2$ ,  $\text{O}_3$ , CO, and VOCs, as shown in Figure 7. During the observation, the total OH reactivity ranged between  $11.46$  and  $29.70 \text{ s}^{-1}$ , with an average of  $19.08 \text{ s}^{-1}$ . In this study, the assessed OH reactivity was significantly higher than those determined in Shanghai, China ( $13.5 \text{ s}^{-1}$ ) (Tan et al., 2018), Beijing, China ( $16.4 \text{ s}^{-1}$ ) (Tan et al., 2019), and Nashville, USA ( $11.3 \text{ s}^{-1}$ ) (Kovacs et al., 2003), but comparable to those in Jinan, China ( $19.4 \text{ s}^{-1}$ ) (Lyu et al., 2019), and London, United Kingdom ( $18.1 \text{ s}^{-1}$ ) (Whalley et al., 2016). This study exclusively calculated the OH reactivity of the measured species, without considering the influence of unmeasured species, such as methane and monoterpenes. Previous research has shown that both unobserved primary emissions and unmeasured secondary products can contribute to unaccounted reactivity (Yang et al., 2016). Consequently, the OH reactivity value determined in this study was slightly underestimated.

$\text{NO}_2$  accounted for the most significant contribution to the overall OH reactivity ( $39.11\%$ ), followed by VOCs ( $28.72\%$ ), NO ( $20.63\%$ ), CO ( $11.05\%$ ),  $\text{SO}_2$  ( $0.33\%$ ), and  $\text{O}_3$  ( $0.16\%$ ), indicating the substantial impact of anthropogenic emissions in Hangzhou (Figure 7). The OH reactivity toward VOCs measured  $5.48 \text{ s}^{-1}$ , which was lower than those observed in Heshan ( $18.3 \text{ s}^{-1}$ ) and Beijing ( $11.2 \text{ s}^{-1}$ ), as reported by Yang et al., in 2017. This phenomenon is attributable to the decreased presence of reactive hydrocarbons, such as aromatics and alkenes, as well as unmeasured species (e.g., 2/3-pentanone), in this study. Alkenes were the primary contributor to the total reactivity of VOCs toward OH ( $44.07\%$ ), followed by OVOCs ( $31.78\%$ ), aromatics ( $14.34\%$ ), alkanes ( $9.63\%$ ), and alkynes ( $0.18\%$ ). Regarding OH reactivity toward specific VOC species, the top 10 species were as follows: 1-butene, hexanal, ethanal, propionaldehyde, 1,3-butadiene, trans-2-butene, propylene, ethene, m-xylene, and toluene. Despite comprising only  $29.56\%$  of the total VOC concentrations, these species collectively accounted for  $68.17\%$  of the total reactivity of the VOCs toward OH, consistent with the findings of Yang et al. (2020).

The OH reactivity displayed notable seasonal fluctuations, as depicted in Supplementary Figure S3. Statistical analysis revealed that the average OH reactivity values followed the order of winter ( $24.20 \text{ s}^{-1}$ ) > spring ( $19.22 \text{ s}^{-1}$ ) > autumn ( $18.07 \text{ s}^{-1}$ ) > summer ( $14.86 \text{ s}^{-1}$ ). These significant variations are attributable to increased concentrations of reactive trace gases, particularly  $\text{NO}_x$  and VOCs. In addition to meteorological factors, combustion during the heating season in Hangzhou produced higher concentrations of  $\text{NO}_x$  and VOCs, consequently leading to higher OH reactivity. Therefore, it is imperative to consistently reinforce policies for controlling trace gases, particularly during the winter season. Regarding the seasonal variations in OH reactivity of VOCs, the highest value was observed in spring ( $6.20 \text{ s}^{-1}$ ), while the lowest value was in autumn ( $4.30 \text{ s}^{-1}$ ). However, the concentrations of key species varied significantly among the four seasons. In general, the research on specific OH reactivity reveals seasonal variations in major reactants. Therefore, OH reactivity-based control strategies should prioritize these key species.

#### 3.3.2 Impact of VOCs on ozone formation

Atmospheric VOCs play a crucial role as  $\text{O}_3$  precursors owing to their photochemical reactivity (Kumar et al., 2018). Figure 8 displays the

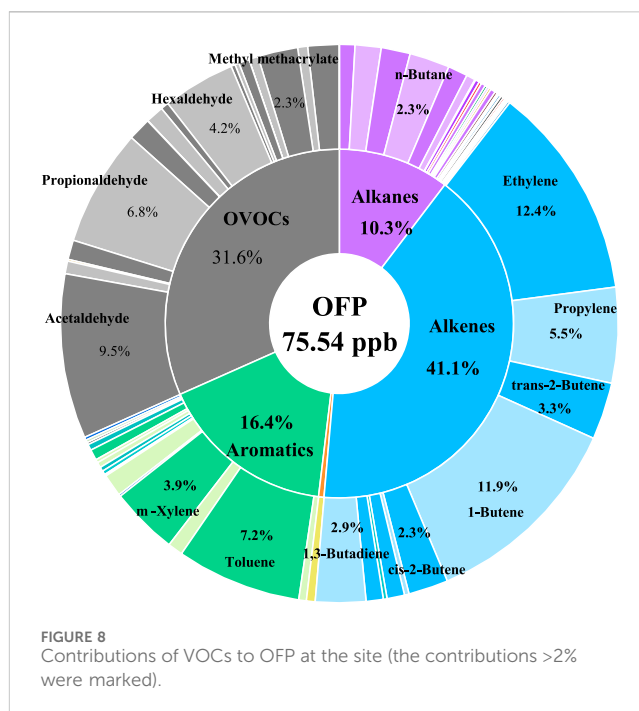
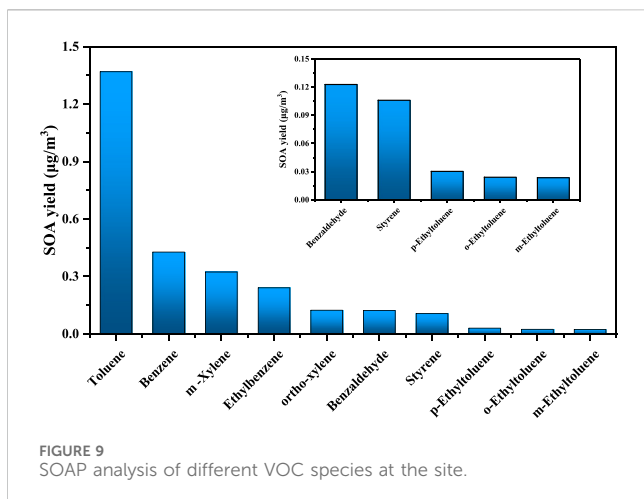


FIGURE 8 Contributions of VOCs to OFP at the site (the contributions >2% were marked).

proportions of OFP contributions from primary VOC categories and species. In this study, the OFP measured at the ZT site was  $75.54 \text{ ppb}$  for VOCs. We show strong seasonal variability in OFP of VOCs followed the order of spring ( $83.05 \text{ ppb}$ ) > summer ( $79.42 \text{ ppb}$ ) > winter ( $78.44 \text{ ppb}$ ) > autumn ( $60.43 \text{ ppb}$ ). The  $\text{O}_3$  contribution attributed to VOCs was lower than those observed in Hangzhou, China (Jing et al., 2020a), and Delhi, India (Kumar et al., 2018). The primary contributor to the OFP was alkenes, particularly ethylene and butene, which displayed significant photochemical reactivity, accounting for  $41.06\%$  of the OFP. Additionally, OVOCs, notably acetaldehyde and propionaldehyde, exhibited pronounced photochemical reactivity, making them the second most significant contributors to OFP, consistent with the findings of Hui et al., in 2018. Aromatics accounted for  $16.4\%$  of the OFP. These findings indicate a strong correlation between the photochemical reactivity of VOCs and their role in  $\text{O}_3$  formation, consistent with previous research (Guo et al., 2017; Hui et al., 2018; Han et al., 2023). Thus, alkenes and OVOCs were key contributors to  $\text{O}_3$  formation. According to the previously discussed PMF results, emissions from vehicles and combustion, identified as primary sources at the sampling sites, should be prioritized for control measures.

#### 3.3.3 SOA formation potential

The strong associations between VOCs and new particle formation have prompted a quantitative discussion on SOAP, with Derwent's methodology widely endorsed as the standard reference (Derwent et al., 2010). SOAP was calculated as  $2.92 \mu\text{g m}^{-3}$  for the VOCs measured at the sampling site. This result was higher than those obtained for Shanghai, China ( $1.00 \mu\text{g m}^{-3}$ ) (Han et al., 2023), and Nanjing, China ( $0.36 \mu\text{g m}^{-3}$ ) (Mozaffar et al., 2020). The SOAP values accounted for  $8.55\%$  of the  $\text{PM}_{2.5}$  concentrations (SOAP values/ $\text{PM}_{2.5}$  concentrations), which was lower than the result for Wangdu, China ( $17.84\%$  under low- $\text{NO}_x$  conditions) (Zhang et al., 2020) and higher than the result for Nanjing, China ( $3.46\%$ ) (Mozaffar et al., 2020). Aromatics were identified as the primary contributors to SOA, comprising  $92.73\%$ ,



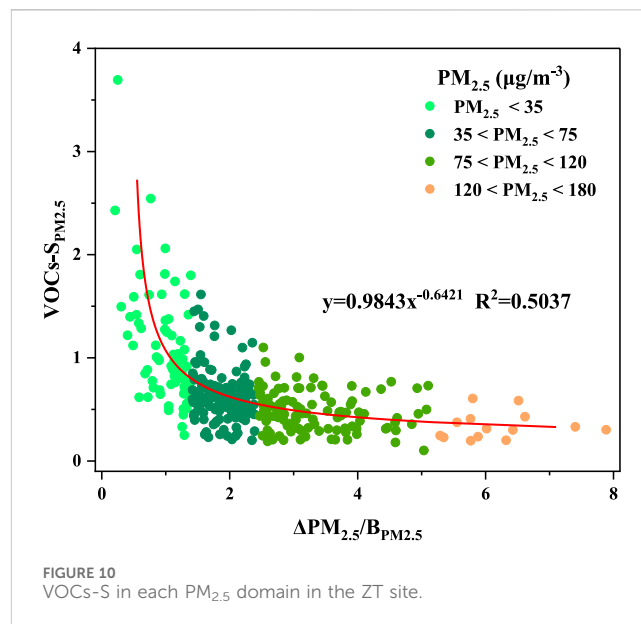
consistent with the findings for Jinan, China (Zhang et al., 2017). The top five VOC species at the sampling site were toluene, benzene, *m*-xylene, ethylbenzene, and *ortho*-xylene (Figure 9). Additionally, the top four SOA-contributing species across all four seasons were toluene, benzene, *m*-xylene and ethylbenzene. Toluene was identified as the most abundant VOC species for SOA formation, with a SOAP value of  $1.37 \mu\text{g m}^{-3}$ . Hence, to enhance SOA reduction outcomes, prioritizing the control of aromatic compound concentrations in Hangzhou is essential, alongside the development of more efficient strategies to curb industrial emissions.

### 3.3.4 Variations in VOCs and $\text{PM}_{2.5}$

Given the close relationship between VOCs and SOA, VOC concentrations respond sensitively to varying levels of  $\text{PM}_{2.5}$  pollution. Therefore, the term “VOCs- $\text{PM}_{2.5}$  sensitivity” ( $\text{VOCs-S}_{\text{PM}_{2.5}}$ ) was employed to elucidate its potential impact on the atmospheric  $\text{PM}_{2.5}$  abundance. Atmospheric pollution here can be categorized into different levels according to the mass concentration of  $\text{PM}_{2.5}$ : clean level ( $\text{PM}_{2.5} < 35 \mu\text{g m}^{-3}$ ), slight pollution level ( $35 < \text{PM}_{2.5} < 75 \mu\text{g m}^{-3}$ ), medium pollution level ( $75 < \text{PM}_{2.5} < 120 \mu\text{g m}^{-3}$ ), and heavy pollution level ( $120 < \text{PM}_{2.5} < 180 \mu\text{g m}^{-3}$ ) (Han et al., 2017; Wang et al., 2022; Han et al., 2023). The changes in  $\text{VOCs-S}_{\text{PM}_{2.5}}$  with  $\text{PM}_{2.5}$  concentration at the sampling site are depicted in Figure 10. The low values of  $\text{VOCs-S}_{\text{PM}_{2.5}}$  generally remained stable with increasing  $\text{PM}_{2.5}$  concentration, while the high values exhibited a declining trend. At the clean level,  $\text{VOCs-S}_{\text{PM}_{2.5}}$  displayed significant variability, spanning from 0.25 to 3.69. However, under the polluted level, particularly during heavy pollution level, the range of  $\text{VOCs-S}_{\text{PM}_{2.5}}$  was narrower, with values oscillating between 0.20 and 0.61. Notably,  $\text{VOCs-S}_{\text{PM}_{2.5}}$  values consistently decreased, while the  $\text{PM}_{2.5}$  to  $B_{\text{PM}_{2.5}}$  ratios increased under clean and slightly polluted level. This trend suggests that VOC concentrations were highly responsive to  $\text{PM}_{2.5}$  levels during the above two episodes.

## 4 Conclusion

In this study, a field observation campaign was conducted at an urban site in Hangzhou throughout the year 2021. The results revealed an average total VOC concentration of 23.60 ppb. The average concentrations of  $\text{O}_3$  and  $\text{PM}_{2.5}$  were  $33.67 \pm 19.68 \mu\text{g m}^{-3}$  and



$34.15 \pm 21.35 \mu\text{g m}^{-3}$ , respectively. Alkanes were the dominant VOC species, constituting 40.13% of the VOC community. During the observation period, the highest VOC concentration was observed in winter (26.49 ppb), followed by spring (23.63 ppb), summer (23.62 ppb), and autumn (20.47 ppb). This phenomenon was attributed to increased atmospheric stability and calm conditions, which limited pollutant dispersion, resulting in higher levels of VOCs during winter.

Special ratios and PMF were employed to examine local sources. The results showed that solvent usage, combustion, and vehicle exhaust were the major VOC sources, accounting for 24.10%, 22.74%, and 19.75%, respectively. According to the 24-h backward trajectory analysis in Hangzhou, the VOC concentration was significantly affected by southeastern air masses prevailing in spring and autumn, eastern air masses dominating in summer, and northwestern air masses being significant in winter.

The OH reactivity, formation potentials of  $\text{O}_3$ , and SOA induced by the studied VOCs were also explored. The campaign-averaged value of total OH reactivity was  $19.08 \text{ s}^{-1}$ , with  $\text{NO}_2$  being the dominant contributor. The OH reactivity of VOCs was  $5.48 \text{ s}^{-1}$ , with alkenes being the dominant contributor (44.07%). The average OFP value was 75.54 ppb, and alkenes and OVOCs played pivotal roles in  $\text{O}_3$  formation. The SOAP averaged  $2.92 \mu\text{g m}^{-3}$ . Aromatics, particularly toluene, were found to be the most abundant VOC species for SOA formation, with a SOAP value of  $1.37 \mu\text{g m}^{-3}$ . VOCs- $\text{PM}_{2.5}$  sensitivity analysis showed that VOCs exhibited greater sensitivity to  $\text{PM}_{2.5}$  on clean level than on level with heavy pollution. Overall, this study provides valuable information into the characteristics of VOCs and contributes to addressing the secondary pollution issue in Hangzhou, China.

## Data availability statement

The original contributions presented in the study are included in the article/Supplementary Material, further inquiries can be directed to the corresponding authors.

## Author contributions

XW: Writing—original draft, Writing—review and editing, Data curation, Investigation, Methodology, Software, Visualization. YH: Writing—original draft, Writing—review and editing, Methodology. XT: Supervision, Writing—review and editing. JS: Data curation, Investigation, Writing—review and editing. BZ: Supervision, Writing—review and editing. HF: Conceptualization, Funding acquisition, Validation, Writing—review and editing.

## Funding

The author(s) declare that financial support was received for the research, authorship, and/or publication of this article. This work was supported by National Key R&D Program of China (grant No. 2022YFC3701102), National Natural Science Foundation of China (grant Nos. 22376029, 22176038, 91744205 and 21777025), and Natural Science Foundation of Shanghai City (grant No. 22ZR1404700).

## References

- Ait-Helal, W., Borbon, A., Sauvage, S., Gouw, J., Colomb, A., Gros, V., et al. (2014). Volatile and intermediate volatility organic compounds in suburban Paris: variability, origin and importance for SOA formation. *Atmos. Chem. Phys. Dis.* 14 (4), 10439–10464. doi:10.5194/acp-14-10439-2014
- An, J., Zhu, B., Wang, H., Li, Y., Lin, X., and Yang, H. (2014). Characteristics and source apportionment of VOCs measured in an industrial area of Nanjing, Yangtze River Delta, China. *Atmos. Environ.* 97, 206–214. doi:10.1016/j.atmosenv.2014.08.021
- An, J. L., Wang, J. X., Zhang, Y. X., and Zhu, B. (2017). Source apportionment of volatile organic compounds in an urban environment at the yangtze river delta, China. *Arch. Environ. Con. Tox.* 72 (3), 335–348. doi:10.1007/s00244-017-0371-3
- Atkinson, R., and Arey, J. (2003). Atmospheric degradation of volatile organic compounds. *Chem. Rev.* 103, 4605–4638. doi:10.1021/cr0206420
- Borbon, A., Gilman, J. B., Kuster, W. C., Grand, N., Chevallier, S., Colomb, A., et al. (2013). Emission ratios of anthropogenic volatile organic compounds in northern mid-latitude megacities: observations versus emission inventories in Los Angeles and Paris. *J. Geophys. Res. Atmos.* 118 (4), 2041–2057. doi:10.1002/jgrd.50059
- Brown, S. G., Eberly, S., Paatero, P., and Norris, G. A. (2015). Methods for estimating uncertainty in PMF solutions: examples with ambient air and water quality data and guidance on reporting PMF results. *Sci. Total Environ.* 518, 626–635. doi:10.1016/j.scitotenv.2015.01.022
- Carter, W. P. L. (1994). Development of ozone reactivity scales for volatile organic compounds. *Air & waste* 44 (7), 881–899. doi:10.1080/1073161x.1994.10467290
- Carter, W. P. L. (1997). *Maximum incremental reactivity excel spreadsheet*.
- Chang, C. X., Wang, J. L., Liu, S. C., and Candice, L. S. C. (2006). Assessment of vehicular and non-vehicular contributions to hydrocarbons using exclusive vehicular indicators. *Atmos. Environ.* 40, 6349–6361. doi:10.1016/j.atmosenv.2006.05.043
- Chen, X., Hopke, P. K., and Carter, W. P. L. (2011). Secondary organic aerosol from ozonolysis of biogenic volatile organic compounds: chamber studies of particle and reactive oxygen species formation. *Environ. Sci. Technol.* 45, 276–282. doi:10.1021/es102166c
- Dechapanaya, W., Eusebi, A., Kimura, Y., and Allen, D. T. (2003). Secondary organic aerosol formation from aromatic precursors. I. Mechanisms for individual hydrocarbons. *Environ. Sci. Technol.* 37, 3662–3670. doi:10.1021/es0209058
- De Gouw, J. A., Middlebrook, A. M., Warneke, C., Ahmadov, R., Atlas, E. L., Bahreini, R., et al. (2011). Organic aerosol formation downwind from the Deepwater Horizon oil spill. *Science* 331 (6022), 1295–1299. doi:10.1126/science.1200320
- Deng, C. X., Jin, Y. J., Zhang, M., Liu, X. W., and Yu, Z. M. (2018). Emission characteristics of VOCs from on-road vehicles in an urban tunnel in eastern China and predictions for 2017–2026. *Aerosol Air Qual. Res.* 18 (12), 3025–3034. doi:10.4209/aaqr.2018.07.0248
- Derwent, R. G., Jenkin, M. E., Utembe, S. R., Shallcross, D. E., Murrells, T. P., and Passant, N. R. (2010). Secondary organic aerosol formation from a large number of

## Conflict of interest

The authors declare that the research was conducted in the absence of any commercial or financial relationships that could be construed as a potential conflict of interest.

## Publisher's note

All claims expressed in this article are solely those of the authors and do not necessarily represent those of their affiliated organizations, or those of the publisher, the editors and the reviewers. Any product that may be evaluated in this article, or claim that may be made by its manufacturer, is not guaranteed or endorsed by the publisher.

## Supplementary material

The Supplementary Material for this article can be found online at: <https://www.frontiersin.org/articles/10.3389/fenvs.2024.1418948/full#supplementary-material>

reactive man-made organic compounds. *Sci. Total Environ.* 408 (16), 3374–3381. doi:10.1016/j.scitotenv.2010.04.013

Dumanoglu, Y., Kara, M., Altiook, H., Odabasi, M., Elbir, T., and Bayram, A. (2014). Spatial and seasonal variation and source apportionment of volatile organic compounds (VOCs) in a heavily industrialized region. *Atmos. Environ.* 98, 168–178. doi:10.1016/j.atmosenv.2014.08.048

Finlayson-Pitts, B. J., and Pitts, J. N. J. (2000) *Chemistry of the upper and lower atmosphere. Theory, experiments, and applications*. New York: Academic Press.

Fu, P., Kawamura, K., Chen, J., and Miyazaki, Y. (2014). Secondary production of organic aerosols from biogenic VOCs over Mt. Fuji, Japan. *Environ. Sci. Technol.* 48, 8491–8497. doi:10.1021/es500794d

Gao, M., Teng, W., Du, Z., Nie, L., An, X., Liu, W., et al. (2021). Source profiles and emission factors of VOCs from solvent-based architectural coatings and their contributions to ozone and secondary organic aerosol formation in China. *Chemosphere* 275, 129815. doi:10.1016/j.chemosphere.2021.129815

Gentner, D. R., Jathar, S. H., Gordon, T. D., Bahreini, R., Day, D. A., Haddad, El, et al. (2017). Review of urban secondary organic aerosol formation from gasoline and diesel motor vehicle emissions. *Environ. Sci. Technol.* 51 (3), 1074–1093. doi:10.1021/acs.est.6b04509

Gu, Y., Liu, B., Li, Y., Zhang, Y., Bi, X., Wu, J., et al. (2020). Multi-scale volatile organic compound (VOC) source apportionment in Tianjin, China, using a receptor model coupled with 1-hr resolution data. *Environ. Pollut.* 265, 115023. doi:10.1016/j.envpol.2020.115023

Gu, Y. Y., Li, Q. Q., Wei, D., Gao, L. R., Tan, L., Su, G. J., et al. (2019). Emission characteristics of 99 NMVOCs in different seasonal days and the relationship with air quality parameters in Beijing, China. *Ecotox. Environ. Safe.* 169, 797–806. doi:10.1016/j.ecoenv.2018.11.091

Guo, H., Cheng, H. R., Ling, Z. H., Louie, P. K. K., and Ayoko, G. A. (2011). Which emission sources are responsible for the volatile organic compounds in the atmosphere of Pearl River Delta? *J. Hazard. Mater.* 188 (1–3), 116–124. doi:10.1016/j.jhazmat.2011.01.081

Guo, H., Ling, Z. H., Cheng, H. R., Simpson, I. J., Lyu, X. P., Wang, X. M., et al. (2017). Tropospheric volatile organic compounds in China. *Sci. Total Environ.* 574, 1021–1043. doi:10.1016/j.scitotenv.2016.09.116

Guo, H., Wang, T., and Louie, P. K. (2004). Source apportionment of ambient non-methane hydrocarbons in Hong Kong: application of a principal component analysis/absolute principal component scores (PCA/APCS) receptor model. *Environ. Pollut.* 129 (3), 489–498. doi:10.1016/j.envpol.2003.11.006

Han, D., Gao, S., Fu, Q., Cheng, J., Chen, X., Xu, H., et al. (2018). Do volatile organic compounds (VOCs) emitted from petrochemical industries affect regional PM<sub>2.5</sub>? *Atmos. Res.* 209, 123–130. doi:10.1016/j.atmosres.2018.04.002

Han, D. M., Wang, Z., Cheng, J. P., Wang, Q., Chen, X. J., and Wang, H. L. (2017). Volatile organic compounds (VOCs) during non-haze and haze days in Shanghai:

- characterization and secondary organic aerosol (SOA) formation. *Environ. Sci. Pollut. Res.* 24, 18619–18629. doi:10.1007/s11356-017-9433-3
- Han, L., Chen, L., Li, K., Bao, Z., Zhao, Y., Zhang, X., et al. (2019). Source apportionment of volatile organic compounds (VOCs) during ozone polluted days in Hangzhou, China. *Atmosphere* 10 (12), 780. doi:10.3390/atmos10120780
- Han, Y., Wang, T., Li, R., Fu, H. B., Duan, Y. S., Gao, S., et al. (2023). Measurement report: volatile organic compound characteristics of the different land-use types in Shanghai: spatiotemporal variation, source apportionment and impact on secondary formations of ozone and aerosol. *Atmos. Chem. Phys.* 23, 2877–2900. doi:10.5194/acp-23-2877-2023
- Huang, C., Wang, H. L., Li, L., Wang, Q., Lu, Q., Gou, De, et al. (2015). VOC species and emission inventory from vehicles and their SOA formation potentials estimation in Shanghai, China. *Atmos. Chem. Phys.* 15 (19), 11081–11096. doi:10.5194/acp-15-11081-2015
- Hui, L., Liu, X., Tan, Q., Feng, M., An, J., Qu, Y., et al. (2018). Characteristics, source apportionment and contribution of VOCs to ozone formation in Wuhan, Central China. *Atmos. Environ.* 192, 55–71. doi:10.1016/j.atmosenv.2018.08.042
- Hui, L., Liu, X., Tan, Q., Feng, M., An, J., Qu, Y., et al. (2019). VOC characteristics, sources and contributions to SOA formation during haze events in Wuhan, Central China. *Sci. Total Environ.* 650, 2624–2639. doi:10.1016/j.scitotenv.2018.10.029
- Jing, S. A., Gao, Y. Q., Shen, J. D., Wang, Q., Peng, Y. R., Li, Y. J., et al. (2020a). Characteristics and reactivity of ambient VOCs in urban Hangzhou, China. *Environ. Sci.* 41 (12), 5306–5315. doi:10.13227/j.hjcx.202004021
- Jing, S. A., Ye, X. H., Gao, Y. Q., Peng, Y. R., Li, Y. J., Wang, Q., et al. (2020b). Characteristics and reactivity during a typical photochemical pollution episode. *Environ. Sci.* 14 (7), 3076–3084. doi:10.13227/j.hjcx.201911187
- Jobson, B. T., Parrish, D. D., Goldan, P., Kuster, W., Fehsenfeld, F. C., Blake, D. R., et al. (1998). Spatial and temporal variability of nonmethane hydrocarbon mixing ratios and their relation to photochemical lifetime. *J. Geophys. Res. Atmos.* 103, 13557–13567. doi:10.1029/97jd01715
- Kovacs, T. A., Brune, W. H., Harder, H., Martinez, M., Simpas, J. B., Frost, G. J., et al. (2003). Direct measurements of urban OH reactivity during Nashville SOS in summer 1999. *J. Environ. Monit.* 5 (1), 68–74. doi:10.1039/b204339d
- Krug, Y., Wang, Y. H., Zhou, P. T., Yao, D., Ji, D. S., Sun, J., et al. (2020). Atmospheric reactivity and oxidation capacity during summer at a suburban site between Beijing and Tianjin. *Atmos. Chem. Phys.* 20, 8181–8200. doi:10.5194/acp-20-8181-2020
- Kumar, A., Singh, D., Kumar, K. S., Singh, B. B., and Jain, V. K. (2018). Distribution of VOCs in urban and rural atmospheres of subtropical India: temporal variation, source attribution, ratios, OFP and risk assessment. *Sci. Total Environ.* 613–614, 492–501. doi:10.1016/j.scitotenv.2017.09.096
- Lai, C., Chuang, K., and Chang, J. (2013). Source apportionment of volatile organic compounds at an international airport. *Aerosol Air Qual. Res.* 13, 689–698. doi:10.4209/aaqr.2012.05.0121
- Li, B., Ho, S. S. H., Li, X., Guo, L., Feng, R., and Fang, X. (2023). Pioneering observation of atmospheric volatile organic compounds in Hangzhou in eastern China and implications for upcoming 2022 Asian Games. *J. Environ. Sci.* 124, 723–734. doi:10.1016/j.jes.2021.12.029
- Li, M., Zhang, Q., Zheng, B., Tong, D., Lei, Y., Liu, F., et al. (2019a). Persistent growth of anthropogenic non-methane volatile organic compound (NMVOC) emissions in China during 1990–2017: drivers, speciation and ozone formation potential. *Atmos. Chem. Phys.* 19, 8897–8913. doi:10.5194/acp-19-8897-2019
- Li, Q., Su, G., Li, C., Liu, P., Zhao, X., Zhang, C., et al. (2020a). An investigation into the role of VOCs in SOA and ozone production in Beijing, China. *China. Sci. Total Environ.* 720, 137536. doi:10.1016/j.scitotenv.2020.137536
- Lin, H., Wang, M., Duan, Y., Fu, Q., Ji, W., Cui, H., et al. (2020b). O<sub>3</sub> sensitivity and contributions of different NMHC sources in O<sub>3</sub> formation at urban and suburban sites in Shanghai. *Atmosphere* 11 (3), 295. doi:10.3390/atmos11030295
- Ling, Z. H., and Guo, H. (2014). Contribution of VOC sources to photochemical ozone formation and its control policy implication in Hong Kong. *Environ. Sci. Policy.* 38, 180–191. doi:10.1016/j.envsci.2013.12.004
- Ling, Z. H., Guo, H., Cheng, H. R., and Yu, Y. F. (2011). Sources of ambient volatile organic compounds and their contributions to photochemical ozone formation at a site in the Pearl River Delta, southern China. *Environ. Pollut.* 159 (10), 2310–2319. doi:10.1016/j.envpol.2011.05.001
- Ling, Z. H., He, Z. R., Wang, Z., Shao, M., and Wang, X. M. (2019). Sources of methacrolein and methyl vinyl ketone and their contributions to methylglyoxal and formaldehyde at a receptor site in Pearl River Delta. *J. Environ. Sci.* 79, 1–10. doi:10.1016/j.jes.2018.12.001
- Liu, Y., Shao, M., Fu, L. L., Lu, S. H., Zeng, L. M., and Tang, D. G. (2008). Source profiles of volatile organic compounds (VOCs) measured in China: Part I. *Atmos. Environ.* 42 (25), 6247–6260. doi:10.1016/j.atmosenv.2008.01.070
- Liu, Y., Song, M., Liu, X., Zhang, Y., Hui, L., Kong, L., et al. (2020). Characterization and sources of volatile organic compounds (VOCs) and their related changes during ozone pollution days in 2016 in Beijing, China. *Environ. Pollut.* 257, 113599. doi:10.1016/j.envpol.2019.113599
- Liu, Y., Wang, H., Jing, S., Gao, Y., Peng, Y., Lou, S., et al. (2019b). Characteristics and sources of volatile organic compounds (VOCs) in Shanghai during summer: implications of regional transport. *Atmos. Environ.* 215, 116902. doi:10.1016/j.atmosenv.2019.116902
- Liu, Y., Wang, H., Jing, S., Peng, Y., Gao, Y., Yan, R., et al. (2021). Strong regional transport of volatile organic compounds (VOCs) during wintertime in Shanghai megacity of China. *Atmos. Environ.* 244, 117940. doi:10.1016/j.atmosenv.2020.117940
- Louie, P. K., Ho, J. W., Tsang, R. C., Blake, D. R., Lau, A. K., Yu, J. Z., et al. (2013). VOCs and OVOCs distribution and control policy implications in Pearl River Delta region, China. *Atmos. Environ.* 76, 125–135. doi:10.1016/j.atmosenv.2012.08.058
- Lyu, X., Wang, N., Guo, H., Xue, L., Jiang, F., Zeren, Y., et al. (2019). Causes of a continuous summertime O<sub>3</sub> pollution event in Jinan, a central city in the North China Plain. *Atmos. Chem. Phys.* 19 (5), 3025–3042. doi:10.5194/acp-19-3025-2019
- Lyu, X. P., Chen, N., Guo, H., Zhang, W. H., Wang, N., Wang, Y., et al. (2016). Ambient volatile organic compounds and their effect on ozone production in Wuhan, Central China. *Sci. Total Environ.* 541, 200–209. doi:10.1016/j.scitotenv.2015.09.093
- Mao, M., Rao, L. X. T., Jiang, H., He, S. Q., and Zhang, X. L. (2022). Air pollutants in metropolises of eastern coastal China. *Int. J. Environ. Res. Public Health* 19 (22), 15332. doi:10.3390/ijerph192215332
- Mo, Z., Shao, M., Lu, S., Qu, H., Zhou, M., Sun, J., et al. (2015). Process-specific emission characteristics of volatile organic compounds (VOCs) from petrochemical facilities in the Yangtze River Delta, China. *China. Sci. Total Environ.* 533, 422–431. doi:10.1016/j.scitotenv.2015.06.089
- Monod, A., Sive, B. C., Avino, P., Chen, T., Blake, D. R., and Rowland, F. S. (2001). Monoaromatic compounds in ambient air of various cities: a focus on correlations between the xylenes and ethylbenzene. *Atmos. Environ.* 35, 135–149. doi:10.1016/s1352-2310(00)00274-0
- Morrow, N. L. (1990). The industrial production and use of 1,3-butadiene. *Environ. Health Perspect.* 86, 7–8. doi:10.2307/3430925
- Mozaaffar, A., Zhang, Y. L., Fan, M. Y., Cao, F., and Lin, Y. C. (2020). Characteristics of summertime ambient VOCs and their contributions to O<sub>3</sub> and SOA formation in a suburban area of Nanjing, China. *Atmos. Res.* 240, 104923. doi:10.1016/j.atmosres.2020.104923
- Nelson, P. F., and Quigley, S. M. (1983). The m, p-xylenes: ethylbenzene ratio. A technique for estimating hydrocarbon age in ambient atmospheres. *Atmos. Environ.* 17 (3), 659–662. doi:10.1016/0004-6981(83)90141-5
- Paatero, P., and Tapper, U. (1994). Positive matrix factorization: a non-negative factor model with optimal utilization of error estimates of data values. *Environmetrics* 5 (2), 111–126. doi:10.1002/env.3170050203
- Pankow, J. F., Seinfeld, J. H., Asher, W. E., and Erdakos, G. B. (2001). Modeling the formation of secondary organic aerosol. 1. Application of theoretical principles to measurements obtained in the  $\alpha$ -pinene/,  $\beta$ -pinene/, sabinene/,  $\delta^3$ -carene/, and cyclohexene/ozone systems. *Environ. Sci. Technol.* 35, 1164–1172. doi:10.1021/es001321d
- Prinn, R. G. (2003). The cleansing capacity of the atmosphere. *Annu. Rev. Environ. Resour.* 28 (1), 29–57. doi:10.1146/annurev.energy.28.011503.163425
- Qin, J., Wang, X., Yang, Y., Qin, Y., Shi, S., Xu, P., et al. (2021). Source apportionment of VOCs in a typical medium-sized city in North China Plain and implications on control policy. *J. Environ. Sci.* 107, 26–37. doi:10.1016/j.jes.2020.10.005
- Seinfeld, J. H., Erdakos, G. B., Asher, W. E., and Pankow, J. F. (2001). Modeling the formation of secondary organic aerosol (SOA). 2. The predicted effects of relative humidity on aerosol formation in the  $\alpha$ -pinene/,  $\beta$ -pinene/, sabinene/,  $\Delta^3$ -carene/, and cyclohexene/ozone systems. *Environ. Sci. Technol.* 35, 1806–1817. doi:10.1021/es001765+
- Shao, P., An, J. L., Xin, J. Y., Wu, F. K., Wang, J. X., Ji, D. S., et al. (2016). Source apportionment of VOCs and the contribution to photochemical ozone formation during summer in the typical industrial area in the Yangtze River Delta, China. *Atmos. Res.* s176-s177, 64–74. doi:10.1016/j.atmosres.2016.02.015
- Shi, J., Deng, H., Bai, Z., Kong, S., Wang, X., Hao, J., et al. (2015). Emission and profile characteristic of volatile organic compounds emitted from coke production, iron smelt, heating station and power plant in Liaoning Province, China. *Sci. Total Environ.* 515, 101–108. doi:10.1016/j.scitotenv.2015.02.034
- Song, M., Liu, X., Zhang, Y., Shao, M., Lu, K., Tan, Q., et al. (2019). Sources and abatement mechanisms of VOCs in southern China. *Atmos. Environ.* 201, 28–40. doi:10.1016/j.atmosenv.2018.12.019
- Song, M., Tan, Q., Feng, M., Qu, Y., Liu, X., An, J., et al. (2018). Source apportionment and secondary transformation of atmospheric nonmethane hydrocarbons in Chengdu, Southwest China. *J. Geophys. Res. Atmos.* 123 (17), 9741–9763. doi:10.1029/2018jd028479
- Song, M. D., Li, X., Yang, S. D., Yu, X. N., Zhou, S. X., Yang, Y. M., et al. (2021). Spatiotemporal variation, sources, and secondary transformation potential of volatile organic compounds in Xi'an China. *Atmos. Chem. Phys.* 21, 4939–4958. doi:10.5194/acp-21-4939-2021
- Song, Y., Shao, M., Liu, Y., Lu, S., Kuster, W., Goldan, P., et al. (2007). Source apportionment of ambient volatile organic compounds in Beijing. *Environ. Sci. Technol.* 41 (12), 4348–4353. doi:10.1021/es0625982

- Sun, J., Wu, F. K., Hu, B., Tang, G. Q., Zhang, J. K., and Wang, Y. S. (2016). VOC characteristics, emissions and contributions to SOA formation during hazy episodes. *Atmos. Environ.* 141, 560–570. doi:10.1016/j.atmosenv.2016.06.060
- Tan, Z., Lu, K., Jiang, M., Su, R., Dong, H., Zeng, L., et al. (2018). Exploring ozone pollution in Chengdu, southwestern China: a case study from radical chemistry to O<sub>3</sub>-VOC-NO<sub>x</sub> sensitivity. *Sci. Total Environ.* 636, 775–786. doi:10.1016/j.scitotenv.2018.04.286
- Tan, Z., Lu, K., Jiang, M., Su, R., Wang, H., Lou, S., et al. (2019). Daytime atmospheric oxidation capacity in four Chinese megacities during the photochemically polluted season: a case study based on box model simulation. *Atmos. Chem. Phys.* 19 (6), 3493–3513. doi:10.5194/acp-19-3493-2019
- Tong, L., Liao, X., Chen, J., Xiao, H., Xu, L., Zhang, F., et al. (2013). Pollution characteristics of ambient volatile organic compounds (VOCs) in the southeast coastal cities of China. *Environ. Sci. Pollut. Res.* 20 (4), 2603–2615. doi:10.1007/s11356-012-1187-3
- Uttamang, P., Campbell, P. C., Aneja, V. P., and Hanna, A. F. (2020). A multi-scale model analysis of ozone formation in the Bangkok Metropolitan Region, Thailand. *Atmos. Environ.* 229, 117433. doi:10.1016/j.atmosenv.2020.117433
- Vardoulakis, S., Solazzo, E., and Lumberras, J. (2011). Intra-urban and street scale variability of BTEX, NO<sub>2</sub> and O<sub>3</sub> in Birmingham, UK: implications for exposure assessment. *Atmos. Environ.* 45 (29), 5069–5078. doi:10.1016/j.atmosenv.2011.06.038
- Wang, M., Shao, M., Lu, S. H., Yang, Y. D., and Chen, W. T. (2013). Evidence of coal combustion contribution to ambient VOCs during winter in Beijing. *Chin. Chem. Lett.* 24 (9), 829–832. doi:10.1016/j.ccl.2013.05.029
- Wang, Q., Zuo, X., Xia, M., Xie, H., He, F., Shen, S., et al. (2019). Field investigation of temporal variation of volatile organic compounds at a landfill in Hangzhou, China. *Environ. Sci. Pollut. Res.* 26, 18162–18180. doi:10.1007/s11356-019-04917-5
- Wang, S., Zhao, Y., Han, Y., Li, R., Fu, H., Gao, S., et al. (2022). Spatiotemporal variation, source and secondary transformation potential of volatile organic compounds (VOCs) during the winter days in Shanghai, China. *Atmos. Environ.* 286, 119203. doi:10.1016/j.atmosenv.2022.119203
- Whalley, L. K., Stone, D., Bandy, B., Dunmore, R., Hamilton, J. F., Hopkins, J., et al. (2016). Atmospheric OH reactivity in central London: observations, model predictions and estimates of *in situ* ozone production. *Atmos. Chem. Phys.* 16 (4), 2109–2122. doi:10.5194/acp-16-2109-2016
- Xiong, Y., and Du, K. (2020). Source-resolved attribution of ground-level ozone formation potential from VOC emissions in Metropolitan Vancouver, BC. *Sci. Total Environ.* 721, 137698. doi:10.1016/j.scitotenv.2020.137698
- Xu, Z., Huang, X., Nie, W., Chi, X., Xu, Z., Zheng, L., et al. (2017). Influence of synoptic condition and holiday effects on VOCs and ozone production in the Yangtze River Delta region, China. *Atmos. Environ.* 168, 112–124. doi:10.1016/j.atmosenv.2017.08.035
- Yadav, R., Sahu, L., Tripathi, N., Pal, D., Beig, G., and Jaaffrey, S. (2019). Investigation of emission characteristics of NMVOCs over urban site of western India. *Environ. Pollut.* 252, 245–255. doi:10.1016/j.envpol.2019.05.089
- Yamada, H. (2013). Contribution of evaporative emissions from gasoline vehicles toward total VOC emissions in Japan. *Sci. Total Environ.* 449, 143–149. doi:10.1016/j.scitotenv.2013.01.045
- Yan, Y. L., Peng, L., Li, R. M., Li, Y. H., Li, L. J., and Bai, H. L. (2017). Concentration, ozone formation potential and source analysis of volatile organic compounds (VOCs) in a thermal power station centralized area: a study in Shuozhou, China. *Environ. Pollut.* 223, 295–304. doi:10.1016/j.envpol.2017.01.026
- Yang, M., Li, F., Huang, C., Tong, L., Dai, X., and Xiao, H. (2023). VOC characteristics and their source apportionment in a coastal industrial area in the Yangtze River Delta, China. *J. Environ. Sci.* 127, 483–494. doi:10.1016/j.jes.2022.05.041
- Yang, Y., Shao, M., Kefel, S., Li, Y., Lu, K., Lu, S., et al. (2017). How the OH reactivity affects the ozone production efficiency: case studies in Beijing and Heshan, China. *Atmos. Chem. Phys.* 17, 7127–7142. doi:10.5194/acp-17-7127-2017
- Yang, Y., Shao, M., Wang, X., Nölscher, A. C., Kessel, S., Guenther, A., et al. (2016). Towards a quantitative understanding of total OH reactivity: a review. *Atmos. Environ.* 134, 147–161. doi:10.1016/j.atmosenv.2016.03.010
- Yang, Y., Wang, Y. H., Zhou, P. T., Yao, D., Ji, D. S., Sun, J., et al. (2020). Atmospheric reactivity and oxidation capacity during summer at a suburban site between Beijing and Tianjin. *Atmos. Chem. Phys.* 20, 8181–8200. doi:10.5194/acp-20-8181-2020
- Yao, Z., Wu, B., Shen, X., Cao, X., Jiang, X., Ye, Y., et al. (2015). On-road characteristics of VOCs from rural vehicles and their ozone formation potential in Beijing, China. *Atmos. Environ.* 105, 91–96. doi:10.1016/j.atmosenv.2015.01.054
- Ying, F., Bao, Z., Yang, C. J., Yao, L., Zhu, L. Z., and Jiao, L. (2012). Analysis of volatile organic compounds (VOCs) and their atmospheric chemical reactivity in ambient air around urban traffic roads in Hangzhou. *Acta Sci. Circumstantiae* 32 (12), 3056–3064.
- Yu, S., Wang, S., Xu, R., Zhang, D., Zhang, M., Su, F., et al. (2022). Measurement report: intra- and interannual variability and source apportionment of volatile organic compounds during 2018–2020 in Zhengzhou, central China. *Atmos. Chem. Phys.* 22 (22), 14859–14878. doi:10.5194/acp-22-14859-2022
- Zhang, F., Shang, X. N., Chen, H., Xie, G. Z., Fu, Y., Wu, D., et al. (2020b). Significant impact of coal combustion on VOCs emissions in winter in a North China rural site. *Sci. Total Environ.* 720, 137617. doi:10.1016/j.scitotenv.2020.137617
- Zhang, G., Wang, N., Jiang, X., and Zhao, Y. (2017). Characterization of ambient volatile organic compounds (VOCs) in the area adjacent to a petroleum refinery in Jinan, China. *Aerosol Air Qual. Res.* 17 (4), 944–950. doi:10.4209/aaqr.2016.07.0303
- Zhang, G., Xu, H., Qi, B., Du, R., Gui, K., Wang, H., et al. (2018). Characterization of atmospheric trace gases and particulate matter in Hangzhou, China. *Atmos. Chem. Phys.* 18 (3), 1705–1728. doi:10.5194/acp-18-1705-2018
- Zhang, Y., Wang, X., Zhang, Z., Lu, S., Shao, M., Lee, F. S. C., et al. (2013). Species profiles and normalized reactivity of volatile organic compounds from gasoline evaporation in China. *Atmos. Environ.* 79, 110–118. doi:10.1016/j.atmosenv.2013.06.029
- Zhu, L., Payne, V. H., Walker, T. W., Worden, J. R., Jiang, Z., Kulawik, S. S., et al. (2017). PAN in the eastern Pacific free troposphere: a satellite view of the sources, seasonality, interannual variability, and timeline for trend detection. *J. Geophys. Res. Atmos.* 122 (6), 3614–3629. doi:10.1002/2016jd025868
- Zou, Y., Deng, X. J., Zhu, D., Gong, D. C., Wang, H., Li, F., et al. (2015). Characteristics of 1 year of observational data of VOCs, NO<sub>x</sub> and O<sub>3</sub> at a suburban site in Guangzhou, China. *Atmos. Chem. Phys.* 15, 6625–6636. doi:10.5194/acp-15-6625-2015